

# Journal of Geophysical Research: Space Physics

## RESEARCH ARTICLE

10.1029/2018JA025419

### Key Points:

- Only 127 out of 473 EMIC wave events are associated with REP when POES satellites go through the region conjugate to EMIC wave activity
- The coincidence occurrence rate is about 10% higher than the random coincidence occurrence rate
- Proportion of EMIC wave events that are associated with REP: H<sup>+</sup> band and He<sup>+</sup> band waves occurring simultaneously >H<sup>+</sup> band >He<sup>+</sup> band

### Correspondence to:

M. Qin,  
Murong.Qin.GR@dartmouth.edu

### Citation:

Qin, M., Hudson, M., Millan, R., Woodger, L., & Shekhar, S. (2018). Statistical investigation of the efficiency of EMIC waves in precipitating relativistic electrons. *Journal of Geophysical Research: Space Physics*, 123, 6223–6230. <https://doi.org/10.1029/2018JA025419>

Received 9 MAR 2018

Accepted 24 JUN 2018

Accepted article online 30 JUN 2018

Published online 4 AUG 2018

## Statistical Investigation of the Efficiency of EMIC Waves in Precipitating Relativistic Electrons

Murong Qin<sup>1</sup> , Mary Hudson<sup>1</sup>, Robyn Millan<sup>1</sup> , Leslie Woodger<sup>1</sup> , and Sapna Shekhar<sup>1</sup> 

<sup>1</sup>Department of Physics and Astronomy, Dartmouth College, Hanover, NH, USA

**Abstract** Electromagnetic ion cyclotron (EMIC) waves have been proposed to cause relativistic electron precipitation (REP). In our study, we carry out 4 years of analysis from 2013 to 2016, with REP spikes obtained from POES satellites and EMIC waves observation from Van Allen Probes. Among the 473 coincidence events when POES satellites go through the region conjugate to EMIC wave activity, only 127 are associated with REP. Additionally, the coincidence occurrence rate is about 10% higher than the random coincidence occurrence rate, indicating that EMIC waves and relativistic electrons can be statistically related, but the link is weaker than expected. H<sup>+</sup> band EMIC waves have been regarded as less important than He<sup>+</sup> band EMIC waves for the precipitation of relativistic electrons. We demonstrate that the proportion of H<sup>+</sup> band EMIC wave events that are associated with REP (22% to 32%) is slightly higher than for He<sup>+</sup> band EMIC wave activity (18% to 27%). An even greater proportion (25% to 40%) of EMIC waves are accompanied by REP events when H<sup>+</sup> band and He<sup>+</sup> band EMIC waves occur simultaneously.

## 1. Introduction

Electron fluxes in the Earth's trapped radiation environment are highly variable (Reeves et al., 2003; Shen et al., 2017). Wave-particle interactions have been considered to play a critical role in acceleration, loss, and transport processes of the trapped particles (e.g., Thorne, 2010). Particle precipitation into the atmosphere due to pitch angle scattering by waves has been proposed as a significant loss process. Among these waves are electromagnetic ion cyclotron (EMIC) waves (Li et al., 2007; Millan & Thorne, 2007). Quasi-linear diffusion theories showed that strong resonant interactions can scatter relativistic electrons through both cyclotron resonance (Lyons & Thorne, 1972; Ni et al., 2015; Summers & Thorne, 2003; Thorne & Kennel, 1971) and bounce resonance processes (Cao et al., 2017).

EMIC waves are Pc1-Pc2 (0.1–5 Hz; Jacobs et al., 1964) waves below the gyrofrequency of respective ion species (H<sup>+</sup>, He<sup>+</sup>, and O<sup>+</sup>), which support the wave mode in the cold, uniform plasma dispersion relation (Stix, 1962). EMIC waves occur in three distinct bands identified by their frequency range: H<sup>+</sup> band ( $\Omega_{\text{He}}^+ < \omega < \Omega_H^+$ ), He<sup>+</sup> band ( $\Omega_O^+ < \omega < \Omega_{\text{He}}^+$ ), and O<sup>+</sup> band ( $\omega < \Omega_O^+$ ). They are excited by temperature anisotropy ( $T_\perp > T_\parallel$ ) of ring current ions (Jordanova et al., 2008), which usually occurs during geomagnetic storms/substorms (Fraser et al., 2010) or is generated by magnetic compressions (Anderson & Hamilton, 1993; Clausen et al., 2011; Usanova et al., 2012). Simultaneous observation of EMIC waves and relativistic electron precipitation (REP) events has been shown in many previously published case studies. Rodger et al. (2008) presented a case study showing that strong precipitations in a subionospheric monitor are linked to ground-based pulsation measurements of EMIC waves. Miyoshi et al. (2008) observed coincident precipitation of relativistic electrons in the P6 energy channel on board the low altitude polar orbiting NOAA POES-17 satellite that is likely to be caused by He<sup>+</sup> band EMIC waves near the plasmapause. Li et al. (2014) quantitatively analyzed the REP observed by balloon 1G of the first Balloon Array for Radiation Belt Storm Probes Relativistic Electron Losses campaign with closely conjugate EMIC waves observed by a NOAA GOES satellite, demonstrating that He<sup>+</sup> band EMIC waves are likely to account for the REP event studied. A statistical study has also been performed to investigate the proportion of REP events that are associated with EMIC waves. In Hendry et al. (2016), by looking for REP first and then searching for associated waves, it was demonstrated that most POES precipitation-associated EMIC waves occurred in the He<sup>+</sup>/O<sup>+</sup> bands while H<sup>+</sup> band takes up to only 13%. However, the result may be influenced by the fact that there is a lack of H<sup>+</sup> band EMIC waves in ground-based observations due to reflections at the bi-ion hybrid frequency (Erlandson & Anderson, 1996; Johnson & Cheng, 1999; Perraut et al., 1984; Usanova et al., 2008).

While the previous studies showed support for the link between EMIC waves and REP, the quantitative role that EMIC waves play in precipitating relativistic electrons remains an open question. In Blum et al. (2015), it was shown that REP events do not always occur even when conjugate EMIC waves are observed. Further studies are necessary to determine what kind of properties EMIC waves need to precipitate relativistic electrons, understand the properties of EMIC waves that do not cause electron precipitation, and determine how much EMIC waves contribute to the REP.

Here we conduct a statistical study of EMIC wave-driven REP events, adopting wave data from the Van Allen Probes satellites and the particle data from NOAA POES satellites. The percentage of EMIC wave events that are coincident with REP is examined. Random occurrence rate for chance association is checked. The relative importance of H<sup>+</sup> band and He<sup>+</sup> band EMIC waves in scattering relativistic electrons is also compared.

## 2. Observations

### 2.1. Van Allen Probes Observations

Van Allen Probes A and B are two nearly identical spacecraft that were launched into  $\sim 10^\circ$  low-inclination, highly elliptical orbits with an orbital period of  $\sim 9$  hr, a perigee of 600-km height above the Earth's surface, an apogee of  $5.8 R_E$  (Kessel et al., 2013; Mauk et al., 2013). Fluxgate magnetometer in the Electric and Magnetic Field Instrument Suite and Integrated Science (Kletzing et al., 2013) instrument onboard Van Allen Probes A and B can measure the magnetic fields with a frequency range of 0–30 Hz. Applying Fast Fourier Transform method, we obtain the wave frequency spectrum using the 64 vectors/s magnetic field measurements from the fluxgate magnetometer.

### 2.2. Low-Earth Orbit Precipitation Observations

NOAA POES are Sun-synchronous satellites at 800–850 km with a polar orbital period of 100 min. The Medium Energy Proton and Electron Detector onboard the Space Environment Monitor (SEM-2) consists of omnidirectional sensors and four directional detectors (Evans & Greer, 2000). Two of the directional detectors are proton solid-state detectors and the other two are electron solid-state detector telescopes. These telescopes can be classified into a  $0^\circ$  telescope and  $90^\circ$  telescope. The  $0^\circ$  telescope can be used to estimate the precipitation flux (Rodger, Clilverd, et al., 2010). The proton telescope has six energy channels from P1 to P6 and the electron telescope has three energy channels from E1 to E3. Among these channels, the P6 channel is not only sensitive to  $>7,000$ -keV protons but also known to be contaminated by relativistic electrons ( $>700$  keV). The P5 channel is only sensitive to 2,500- to 7,000-keV protons and has no response to electrons at all (Yando et al., 2011). In our study, the full resolution of 2-s data from METOP-1, METOP-2, NOAA-15, NOAA-16, NOAA-18, and NOAA-19 has been adopted to investigate relativistic precipitation events. Measurements in the P5 channel are used to exclude the solar proton events, and the P6 channel is used to identify events and to obtain the precipitated energetic electron count rate.

### 2.3. Statistical Results

We carried out the investigation over 4 years (2013–2016). Adopting magnetic field measurements from the Electric and Magnetic Field Instrument Suite and Integrated Science instrument onboard the Van Allen Probes, EMIC waves were identified by inspection of the frequency spectrum with the following criteria: wave intensity range from  $10^{-2}$  to  $10^5$  (nT)<sup>2</sup>/Hz as enhancements, narrow banded in frequency, and bounded by hydrogen, helium, and oxygen ion cyclotron frequencies between 0 and 12 Hz. EMIC waves are only examined in H<sup>+</sup> and He<sup>+</sup> bands. O<sup>+</sup> band EMIC waves are usually mixed with the broadband background noise and are thus not included in our study. When EMIC waves are observed by both satellites within 1 hr and have similar structure, then they are counted as one EMIC wave event. The events studied in this paper include 394 H<sup>+</sup> band EMIC wave events, 260 He<sup>+</sup> band EMIC wave events, and 74 cases when H<sup>+</sup> and He<sup>+</sup> bands occur simultaneously. An example of an EMIC wave event when H<sup>+</sup> and He<sup>+</sup> bands occur simultaneously is shown in Figure 1.

Spatial scales of EMIC waves have been shown to span from 0.03 to 0.8 hr in magnetic local time (MLT) and 0.02 to 1 in L (Blum et al., 2016). Additionally, spatial scales of REP events are typically less than 0.5 in L and less than 3 hr in MLT when associated with low energy proton precipitation (Shekhar et al., 2017). To keep a close correlation between the REP events observed by POES satellites and any EMIC waves detected by Van Allen Probes, we consider the POES spikes occurring within 20 min before the beginning of the detected EMIC wave and 20 min after the end of the detected EMIC wave since the EMIC wave may still exist before and after the Van Allen Probe spacecraft passes through the wave region. When spacecraft separation is within the span of  $\pm 1$  hr in MLT and  $\pm 1$  in L (McIlwain, 1961), the observations on the two spacecraft are said to be in

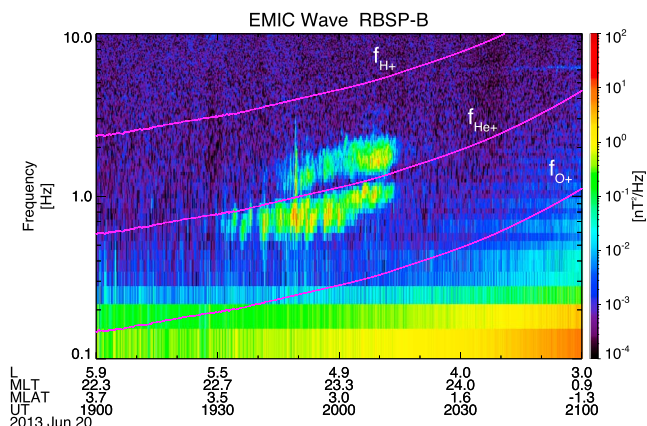


**Figure 1.** An example of EMIC wave event when  $H^+$  and  $He^+$  bands occur simultaneously on 20 June 2013. Superposed pink lines refer to hydrogen ( $H^+$ ), helium ( $He^+$ ), and oxygen ( $O^+$ ) ion gyrofrequencies, which are calculated from magnitude measured by fluxgate magnetometer of the Electric and Magnetic Field Instrument Suite and Integrated Science instrument onboard Van Allen Probes. EMIC = electromagnetic ion cyclotron; RBSP = Radiation Belt Storm Probes.

conjunction. Increases in the POES count rate of the P6 channel greater than 4 c/s are considered as REP events when there is no corresponding increase in the P5 channel. A threshold of 4 c/s was chosen because most of the events with maximum count rate of 4 c/s in the P6 energy channel are noisy single spikes when examined individually. An example of a REP event is shown in Figure 2. Red and black lines represent the count rate in P5 and P6 channels, respectively. In order to avoid being influenced by trapped populations and drift loss cone particles, observations in the vicinity of and inside the South Atlantic Magnetic Anomaly with latitude ranging from  $-52^\circ$  to  $20^\circ$  and longitude ranging from  $-180^\circ$  to  $30^\circ$  are excluded (Qin et al., 2014; Rodger, Carson, et al., 2010). Since EMIC waves usually occurred with disturbed geomagnetic conditions, L values for both Van Allen Probes and POES satellites are both obtained from TS04 models (Tsyganenko & Sitnov, 2005).

The statistical results are shown in Figure 3. Each panel in Figure 3 shows Van Allen Probes A and B combined dwell time in hours, plotted in L-MLT coordinates. Superposed on the Van Allen Probes dwell time in panel (a) are the  $H^+$  band (yellow triangle) EMIC events,  $He^+$  band (white triangle) EMIC events, and  $H^+$  and  $He^+$  band (black triangle) EMIC events when both are seen simultaneously. Panel (b) shows when EMIC wave events are observed by Van Allen Probes in conjunction with available POES measurements. In Figure 3c, REP events are observed by POES in conjunction with  $H^+$  (yellow),  $He^+$  (white), and both bands (black) of EMIC waves observed by Van Allen Probes. There are a total of 473 cases when EMIC wave events observed by Van Allen Probes are in conjunction with available POES measurements, with 251  $H^+$  band, 166  $He^+$  band, and 56 both bands EMIC wave events, respectively. Among the total 473 conjunction events, only 127 are associated with REP, with 68 of them being  $H^+$  band EMIC waves, 42 being  $He^+$  band EMIC waves, and the remaining 17 being

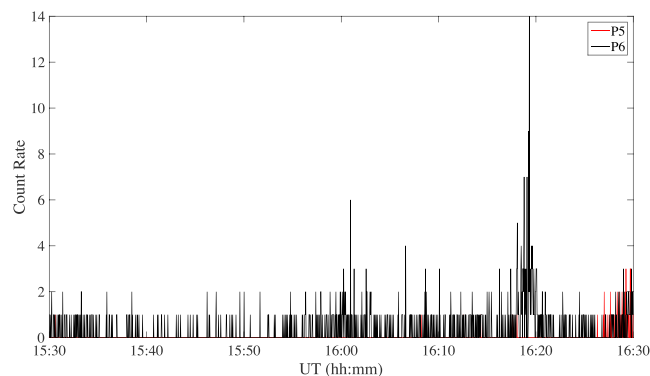


**Figure 2.** An example of relativistic electron precipitation at 16:20 UT on 27 August 2015. Spike at 16:01 UT is also counted as a relativistic electron precipitation event in the statistical study. Red and black lines represent the count rate in P5 and P6 channel, respectively.

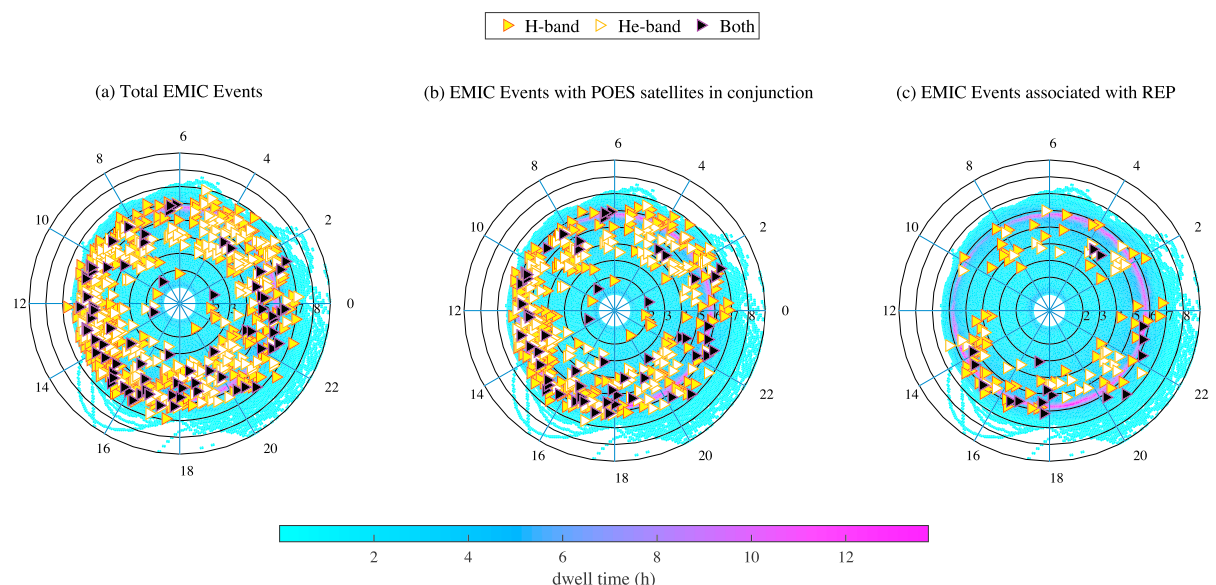


**Figure 3.** (a) Van Allen Probes A and B combined dwell time in hours, plotted in L-MLT coordinates. The color spectrum is the dwell time of Van Allen Probes, and the concentric purple ring is where Van Allen Probes spend the most time. Superposed are the H<sup>+</sup> band (yellow triangle) EMIC events, He<sup>+</sup> band (white triangle) EMIC events, and H<sup>+</sup> and He<sup>+</sup> band (black triangle) EMIC events. (b) H<sup>+</sup> (yellow), He<sup>+</sup> (white), and both bands of EMIC events (black) with POES conjunction in MLT-L location plotted. (c) The superposed triangles on the dwell time are REP events associated with H<sup>+</sup> (yellow), He<sup>+</sup> (white), and both bands (black) of EMIC waves. EMIC = electromagnetic ion cyclotron; REP = relativistic electron precipitation; MLT = magnetic local time.

EMIC waves when both bands are observed simultaneously. It can be calculated that 27.1% of H<sup>+</sup> band EMIC waves, 25.3% of He<sup>+</sup> band EMIC waves, and 30.3% of the cases with both bands being observed are associated with REP events when POES satellites go through the region of EMIC wave activity observed by Van Allen Probes. Most coincidence events lie beyond L > 3. H<sup>+</sup> band EMIC waves associated with REP events have a maximum in 12–18 MLT. He<sup>+</sup> band EMIC waves associated with REP events have a maximum from 18 to 22 MLT and 2 to 4 MLT. The coincidence events from 2 to 4 MLT mostly lie in the H<sup>+</sup> band.

To examine the effect of restriction of conjunction in time and space on the occurrence rate of EMIC associated REP events, we further extend our analysis for a set of  $\Delta L$  and  $\Delta MLT$  between POES and one Van Allen Probe spacecraft, with  $\Delta L$  ranging from  $\pm 0.1$  to  $\pm 1.5$  and  $\Delta MLT$  from  $\pm 0.1$  to  $\pm 1.5$  (Figure 4a). There is also a possibility that the coincident EMIC wave events and REP events are uncoupled and just happen to occur simultaneously, which will lead to an overestimation of the efficiency of EMIC waves in precipitating relativistic electrons. In order to test for the random coincidence, we calculate the occurrence rate of REP at the same location of each coincidence event with a shifted window of  $\pm 15$  days, that is, REP occurs at the same temporal and spatial region as the coincident events, but with the corresponding EMIC wave event happening 15 days later or in advance (Figures 4b and 4c). It can be seen that the coincidence occurrence rate becomes progressively larger when we expand the restriction criterion, with the maximum value of 31.18%, which is about 10% higher than the peak value of random coincidence when a REP event occurs independently 15 days before or after an EMIC wave event. Additionally, the coincidence occurrence rate is higher than the random coincidence overall, with the exact coincidence exceeding the chance associations at about 10% when there are adequate samples for good statistics with conjunction criterion  $\Delta L$  ranging from  $\pm 0.7$  to  $\pm 1.5$ . The above result suggests that while the peak coincidence occurrence rate goes to 31.18%, the chance coincidence may influence the statistics. The actual coincidence rate exceeds the random coincidence occurrence rate in all cases suggesting a correlation between REP and EMIC waves. However, a consistently low percentage of EMIC waves that are possible to drive REP events is found for all the spacecraft separations examined.

A similar method is then applied for assessing the relative importance of different bands of EMIC waves in scattering relativistic electrons. Figure 5 shows the result of the coincidence occurrence rate with REP events for H<sup>+</sup> band (a), He<sup>+</sup> band (b), and when both bands occur simultaneously (c). From Figure 5, it can be seen that for conjunction restrictions with  $\Delta L$  ranging from  $\pm 0.7$  to  $\pm 1.5$  and  $\Delta MLT$  ranging from  $\pm 0.4$  to  $\pm 1.5$ , the coincidence occurrence rate with REP events for H<sup>+</sup> band and He<sup>+</sup> band EMIC waves occurring simultaneously is greater than the cases when only H<sup>+</sup> band or He<sup>+</sup> band EMIC waves occur. Additionally, the coincidence

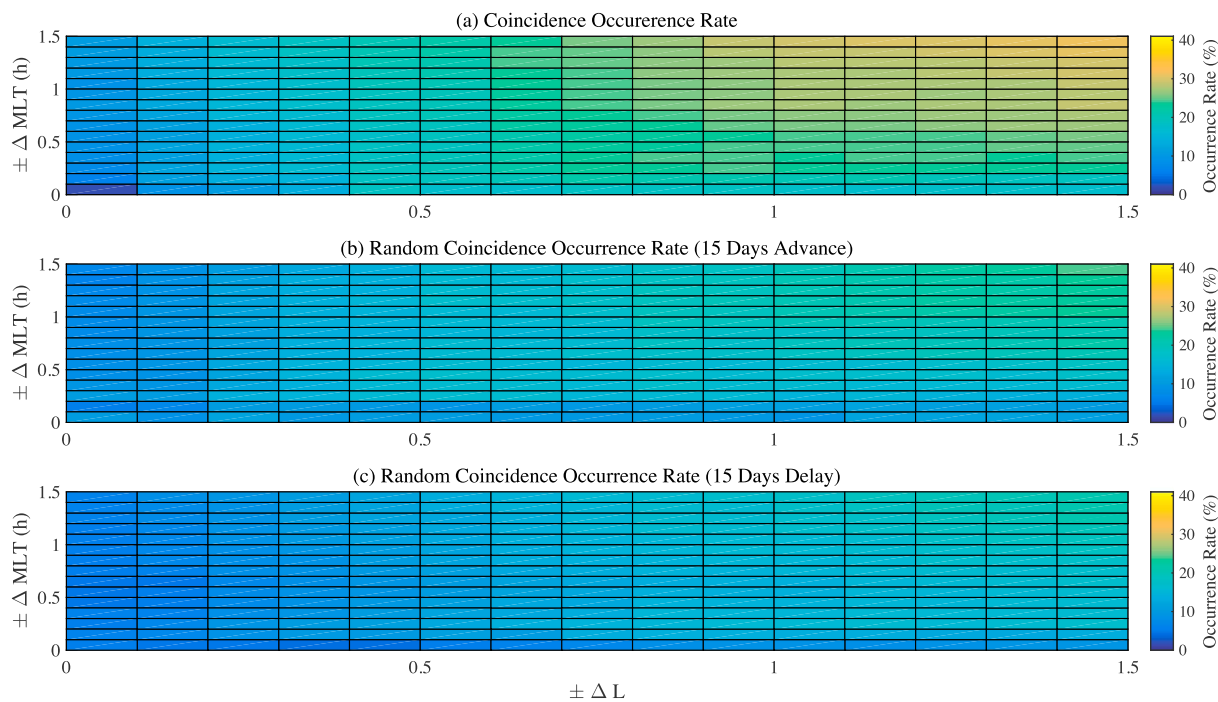


**Figure 4.** (a) The coincidence occurrence rate of REP observed by POES satellites when passing through EMIC event activity, spacecraft separation in MLT ranging from  $\pm 0.1$  to  $\pm 1.5$ , and separation in L ranging from  $\pm 0.1$  to  $\pm 1.5$ . REP occurring within 20 min before the beginning and 20 min after the end of the EMIC activities are included. (b) The random coincidence occurrence rate of REP observed by POES satellites when it pass through the same temporal and spatial region as in panel (a) of the EMIC waves that happens 15 days later. (c) Same as panel (a), but with EMIC wave activity happens 15 days before the corresponding REP event. EMIC = electromagnetic ion cyclotron; REP = relativistic electron precipitation; MLT = magnetic local time.

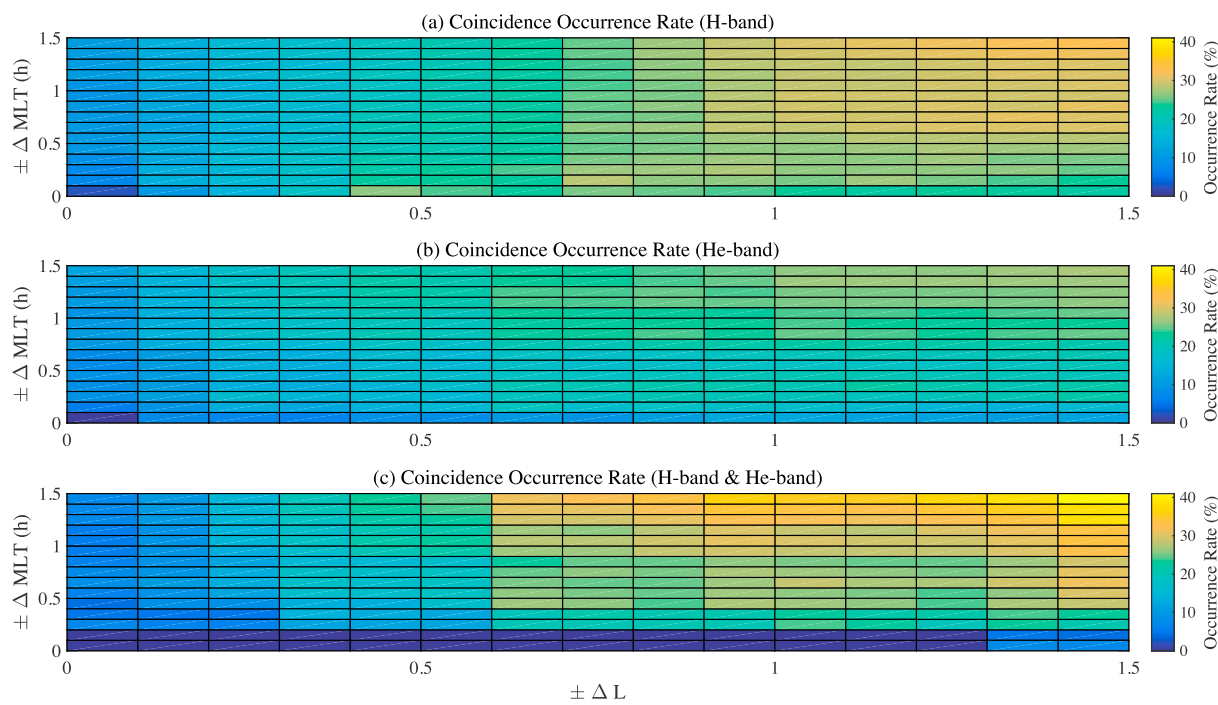


**Figure 5.** (a) The proportion of the time that relativistic electron precipitation events occurs when  $H^+$  band power was observed on Van Allen Probes-POES conjunctions, spacecraft separation in MLT ranging from  $\pm 0.1$  to  $\pm 1.5$  and separation in L ranging from  $\pm 0.1$  to  $\pm 1.5$ . Relativistic electron precipitation occurs within 20 min before the beginning and 20 min after the end of the EMIC activities are included. (b) Same as panel (a), but for  $He^+$  band EMIC wave activity. (c) Same as panel (a), but for  $H^+$  band and  $He^+$  band EMIC wave activities occurring simultaneously. EMIC = electromagnetic ion cyclotron; MLT = magnetic local time.

occurrence rate with REP events for H<sup>+</sup> band EMIC waves is slightly higher than the He<sup>+</sup> band waves overall. The REP events occur 22.51% to 32.17% of the time when H<sup>+</sup> band power was observed on Van Allen Probes-POES conjunctions, 18.51% to 27.00% of the time that He<sup>+</sup> band was available and 25.00% to 40.57% of the time when H<sup>+</sup> band and He<sup>+</sup> band EMIC waves occur simultaneously. For the conjunction criterion listed above, the random coincidence occurrence rate for each kind of band with ±15 days shifted is also examined (not shown) and turns out to have comparable values to the random coincidence occurrence rate with all the bands checked together in Figures 4b and 4c.

### 3. Discussion and Summary

In this paper, we obtain precipitation spikes from a series of POES satellites correlated with EMIC wave observations from Van Allen Probes, performing statistical investigation of the efficiency of H<sup>+</sup> and He<sup>+</sup> band EMIC waves in driving the REP. We check the coincidence occurrence rate when EMIC waves are associated with REP events and the random coincidence occurrence rate when REP is observed in the same spatial region as EMIC waves but with each corresponding EMIC wave event occurring 15 days earlier and later to test the statistical correlation between EMIC waves and REP events.

A consistently low percentage of observed EMIC waves were associated with REP events for all the space-craft separations examined, with the peak coincidence occurrence rate reaching 31.18%. The coincidence event occurrence rate when conjunction REP events and EMIC wave activity occurs simultaneously is about 10% higher than chance associations overall. On the one hand, these results show that EMIC waves and REP events may be causally related. On the other hand, the above results suggest that while the peak coincidence occurrence rate goes to 31.18%, the chance coincidence may influence the statistics. More attention should be given in determining whether they are causally related when there are conjugate observations of REP and EMIC wave activity in future planned event studies.

The relative importance of different bands of EMIC waves in scattering relativistic electrons is also assessed in our paper. It is shown that coincidence occurrence rates for different bands are all higher than the random coincidence occurrence rate, which further demonstrates that both H<sup>+</sup> band and He<sup>+</sup> band EMIC waves may be causally related with REP events. Hendry et al. (2016) showed that most POES precipitation-associated EMIC waves occurred in the He<sup>+</sup>/O<sup>+</sup> band by looking for REP first and then searching for associated EMIC waves. However, this does not imply greater difficulty for H<sup>+</sup> band EMIC waves to scatter relativistic electrons into the loss cone, but rather may be due to the absence of H<sup>+</sup> band EMIC waves detected on the ground (Erlandson & Anderson, 1996; Johnson & Cheng, 1999; Perraut et al., 1984; Usanova et al., 2008). We do the reverse in our statistical result by investigating EMIC waves first and then exploring the associated REP events. The EMIC waves detected by Van Allen Probes instead of ground observation avoid the transmission of waves through the ionosphere and their subsequent ducting in the ionospheric F2 region waveguide, which can distribute EMIC waves up to over a thousand or more kilometers from the source field line footprint (Althouse & Davis, 1978; Fraser, 1975). It is shown that the proportion of H<sup>+</sup> band EMIC wave events that are associated with REPs is slightly higher than He<sup>+</sup> band EMIC waves. We also carried out the analysis for a narrower 20-min window (10 min before the beginning of the detected EMIC wave and 10 min after the end of the detected EMIC wave) and found similar results (not shown). It is important to note the difference even though the coincidence occurrence rate is only slightly higher for H<sup>+</sup> band EMIC waves than He<sup>+</sup> band EMIC waves, since H<sup>+</sup> band EMIC waves have generally been regarded as less important than He<sup>+</sup> band EMIC waves, which mostly occur on the duskside correlated with high background plasma density in many prior studies (Fraser et al., 2010; Min et al., 2012). Higher background plasma density has been shown to reduce the minimum energy required for cyclotron resonance and pitch angle scattering (Summers & Thorne, 2003). The higher coincidence occurrence rate for H<sup>+</sup> band in our result suggests that, besides the background plasma density, other parameters such as the wave normal angle and the normalized wave frequency in each band might also have an influence on the efficiency of EMIC waves in scattering relativistic electrons.

It should also be noted that we found a greater proportion of EMIC waves that are associated with REP events when H<sup>+</sup> band and He<sup>+</sup> band occurs simultaneously. This could be a result of insufficient samples of EMIC waves when H<sup>+</sup> band and He<sup>+</sup> band occurs simultaneously, or could indicate that there are circumstances when H<sup>+</sup> band waves exist but the local plasma environment is only favorable for electron resonance with He<sup>+</sup> band EMIC waves or vice versa. Thus, we cannot easily tell which band of EMIC waves most effectively scatters relativistic electrons from our coincidence study alone. Complex factors, such as local background plasma

conditions, the initial electron pitch angle, and energy-flux distributions, as well as the wave frequency and amplitude in each propagation band play an intricate role in determining resonance with relativistic electrons. The weaker geomagnetic activity compared to the previous solar maximum (Halford et al., 2010) and the especially lower intensities of electrons in the radiation belt in the year 2013 might be a potential bias for the low percentage of EMIC waves associated with REP events in this study. Besides, as the initial electron population is significantly affected by the wave-particle interaction, it is possible that the trapped population may have already been depleted before POES satellites pass through the wave activity region, which may lead to an underestimation of the coincidence rate. An in-depth study will be performed in future work to test the causality between EMIC waves and REP events and check the role that these factors and other potential influences play in determining the ability of EMIC waves to precipitate relativistic electrons.

### Acknowledgments

This work was supported by NASA grant NNX15AF54G and JHU/APL under NASA contracts NNN16AA09T and NNN06AA01C to UMN and UNH with subcontracts to Dartmouth. The Van Allen Probe EMFISIS data can be obtained at <https://emfisis.physics.uiowa.edu/data/index>, and POES satellite data can be downloaded from <https://www.ngdc.noaa.gov/stp/satellite/poes/dataaccess.html>.

### References

- Althouse, E. L., & Davis, J. R. (1978). Five-station observations of Pc 1 micropulsation propagation. *Journal of Geophysical Research*, 83(A1), 132–144. <https://doi.org/10.1029/JA083iA01p00132>
- Anderson, B. J., & Hamilton, D. C. (1993). Electromagnetic ion cyclotron waves stimulated by modest magnetospheric compressions. *Journal of Geophysical Research*, 98(A7), 11,369–11,382. <https://doi.org/10.1029/93JA00605>
- Blum, L., Agapitov, O., Bonnell, J., Kletzing, C., & Wygant, J. (2016). EMIC wave spatial and coherence scales as determined from multipoint Van Allen Probe measurements. *Geophysical Research Letters*, 43, 4799–4807. <https://doi.org/10.1002/2016GL068799>
- Blum, L. W., Halford, A., Millan, R., Bonnell, J. W., Goldstein, J., Usanova, M., et al. (2015). Observations of coincident EMIC wave activity and duskside energetic electron precipitation on 18–19 January 2013. *Geophysical Research Letter*, 42, 5727–5735. <https://doi.org/10.1002/2015GL065245>
- Cao, X., Ni, B., Summers, D., Tao, X., Shprits, Y. Y., et al. (2017). Bounce resonance scattering of radiation belt electrons by H<sup>+</sup> band EMIC waves. *Journal of Geophysical Research: Space Physics*, 122(2), 1702–1713. <https://doi.org/10.1002/2016JA023607>
- Clausen, L., Baker, J., Ruohoniemi, J., & Singer, H. (2011). EMIC waves observed at geosynchronous orbit during solar minimum: Statistics and excitation. *Journal of Geophysical Research*, 116(A10). <https://doi.org/10.1029/2011JA016823>
- Erlandson, R. E., & Anderson, B. J. (1996). Pc 1 waves in the ionosphere: A statistical study. *Journal of Geophysical Research*, 101(A4), 7843–7857. <https://doi.org/10.1029/96JA00082>
- Evans, D. S., & Greer, M. S. (2000). Polar orbiting environmental satellite space environment. Monitor-2: Instrument Description and Archive Data Documentation.
- Fraser, B. J. (1975). Ionospheric duct propagation and Pc 1 pulsation sources. *Journal of Geophysical Research*, 80(19). <https://doi.org/10.1029/JA080i019p02790>
- Fraser, B., Grew, R., Morley, S., Green, J., Singer, H., Loto'aniu, T., & Thomsen, M. (2010). Storm time observations of electromagnetic ion cyclotron waves at geosynchronous orbit: GOES results. *Journal of Geophysical Research: Space Physics*, 115(A5). <https://doi.org/10.1029/2009JA014516>
- Halford, A. J., Fraser, B. J., & Morley, S. K. (2010). EMIC wave activity during geomagnetic storm and nonstorm periods: CRRES results. *Journal of Geophysical Research*, 115(A12248), A12248. <https://doi.org/10.1029/2010JA015716>
- Hendry, A., Rodger, C., Clilverd, M., Engebretson, M., Mann, I., Lessard, M., et al. (2016). Confirmation of EMIC wave-driven relativistic electron precipitation. *Journal of Geophysical Research: Space Physics*, 121(6), 5366–5383. <https://doi.org/10.1002/2015JA022224>
- Jacobs, J. A., Kato, Y., Matsushita, S., & Troitskaya, V. A. (1964). Classification of geomagnetic micropulsations. *Journal of Geophysical Research*, 69(1), 180–181. <https://doi.org/10.1029/JZ069i001p00180>
- Johnson, J. R., & Cheng, C. (1999). Can ion cyclotron waves propagate to the ground? *Geophysical Research Letters*, 26(6), 671–674.
- Jordanova, V., Albert, J., & Miyoshi, Y. (2008). Relativistic electron precipitation by EMIC waves from self-consistent global simulations. *Journal of Geophysical Research: Space Physics*, 113(A3). <https://doi.org/10.1029/2008JA013239>
- Kessel, R., Fox, N., & Weiss, M. (2013). The Radiation Belt Storm Probes (RBSP) and space weather. *Space Science Reviews*, 179, 531–543. <https://doi.org/10.1007/s11214-012-9953-6>
- Kletzing, C., Kurth, W., Acuna, M., MacDowall, R. J., Torbert, R. B., Averkamp, T., et al. (2013). The Electric and Magnetic Field Instrument Suite and Integrated Science (EMFISIS) on RBSP. *Space Science Review*, 179(1–4), 127–181. <https://doi.org/10.1007/s11214-013-9993-6>
- Li, W., Shprits, Y. Y., & Thorne, R. M. (2007). Dynamic evolution of energetic outer zone electrons due to wave-particle interactions during storms. *Journal of Geophysical Research*, 112, A10220. <https://doi.org/10.1029/2007JA012368>
- Li, Z., Millan, R., Hudson, M., Woodger, L., Smith, D., Chen, Y., et al. (2014). Investigation of EMIC wave scattering as the cause for the BARREL 17 January 2013 relativistic electron precipitation event: A quantitative comparison of simulation with observations. *Geophysical Research Letter*, 41, 8722–8729. <https://doi.org/10.1002/2014GL062273>
- Lyons, L. R., & Thorne, R. M. (1972). Parasitic pitch angle diffusion of radiation belt particles by ion cyclotron waves. *Journal of Geophysical Research*, 77(28), 5608–5616. <https://doi.org/10.1029/JA077i028p05608>
- Mauk, B., Fox, N., Kanekal, S., Kessel, R., Sibeck, D., & Ukhorskiy, A. (2013). Science objectives and rationale for the Radiation Belt Storm Probes mission. *Space Science Review*, 179(1–4), 3–27. <https://doi.org/10.1007/s11214-012-9908-y>
- McIlwain, C. E. (1961). Coordinates for mapping the distribution of magnetically trapped particles. *Journal of Geophysical Research*, 66(11), 3681–3691.
- Millan, R., & Thorne, R. (2007). Review of radiation belt relativistic electron losses. *Journal of Atmospheric and Solar-Terrestrial Physics*, 69(3), 362–377. <https://doi.org/10.1016/j.jastp.2006.06.019>
- Min, K., Lee, J., Keika, K., & Li, W. (2012). Global distribution of EMIC waves derived from THEMIS observations. *Journal of Geophysical Research: Space Physics*, 117, A05219. <https://doi.org/10.1029/2012JA017515>
- Miyoshi, Y., Sakaguchi, K., Shiokawa, K., Evans, D., Albert, J., Connors, M., & Jordanova, V. (2008). Precipitation of radiation belt electrons by EMIC waves, observed from ground and space. *Geophysical Research Letters*, 35. <https://doi.org/10.1029/2008GL035727>
- Ni, B., Cao, X., Zou, Z., Zhou, C., Gu, X., Bortnik, J., et al. (2015). Resonant scattering of outer zone relativistic electrons by multi-band EMIC waves and resultant electron loss time scales. *Journal of Geophysical Research: Space Physics*, 120(9), 7357–7373. <https://doi.org/10.1002/2015JA021466>
- Perraut, S., Gendrin, R., Roux, A., & de Villedary, C. (1984). Ion cyclotron waves: Direct comparison between ground-based measurements and observations in the source region. *Journal of Geophysical Research*, 89(A1), 195–202. <https://doi.org/10.1029/JA089iA01p00195>

- Qin, M., Zhang, X., Ni, B., Song, H., Zou, H., & Sun, Y. (2014). Solar cycle variations of trapped proton flux in the inner radiation belt. *Journal of Geophysical Research: Space Physics*, 119(12), 9658–9669. <https://doi.org/10.1002/2014JA020300>
- Reeves, G. D., McAdams, K. L., Friedel, R. H. W., & O'Brien, T. P. (2003). Acceleration and loss of relativistic electrons during geomagnetic storms. *Geophysical Research Letters*, 30(10), 1529. <https://doi.org/10.1029/2002GL016513>
- Rodger, C., Clilverd, M., Green, J., & Lam, M. (2010). Use of POES SEM-ÅR2 observations to examine radiation belt dynamics and energetic electron precipitation into the atmosphere. *Journal Geophysical Research: Space Physics*, 115, A04202. <https://doi.org/10.1029/2008JA014023>
- Rodger, C., Raita, T., Clilverd, M., Seppälä, A., Dietrich, S., Thomson, N., & Ulich, T. (2008). Observations of relativistic electron precipitation from the radiation belts driven by EMIC waves. *Geophysical Research Letter*, 35, L16106. <https://doi.org/10.1029/2008GL034804>
- Rodger, C. J., Carson, B. R., Cummer, S. A., Gamble, R. J., Clilverd, M. A., Green, J. C., et al. (2010). Contrasting the efficiency of radiation belt losses caused by ducted and nonducted whistler-mode waves from ground-based transmitters. *Journal of Geophysical Research*, 115(A4), a12208. <https://doi.org/10.1029/2010JA015880>
- Shekhar, S., Millan, R., & Smith, D. (2017). A statistical study of the spatial extent of relativistic electron precipitation with polar orbiting environmental satellites. *Journal Geophysical Research: Space Physics*, 122, 11,274–11,284. <https://doi.org/10.1002/2017JA024716>
- Shen, X.-C., Hudson, M. K., Jaynes, A., Shi, Q., Tian, A., Claudepiere, S., et al. (2017). Statistical study of the storm time radiation belt evolution during Van Allen Probes era: CME- versus CIR-driven storms. *Journal Geophysical Research: Space Physics*, 122, 8327–8339. <https://doi.org/10.1002/2017JA024100>
- Stix, T. H. (1962). *The theory of plasma waves*. New York: McGraw-Hill, pp. 1962.
- Summers, D., & Thorne, R. (2003). Relativistic electron pitch-angle scattering by electromagnetic ion cyclotron waves during geomagnetic storms. *Journal Geophysical Research: Space Physics*, 108(A4), 1143. <https://doi.org/10.1029/2002JA009489>
- Thorne, R. M. (2010). Radiation belt dynamics: The importance of wave-particle interactions. *Geophysical Research Letter*, 37(22), L22107. <https://doi.org/10.1029/2010GL044990>
- Thorne, R. M., & Kennel, C. (1971). Relativistic electron precipitation during magnetic storm main phase. *Journal Geophysical Research*, 76(19), 4446–4453. <https://doi.org/10.1029/JA076i019p04446>
- Tsyganenko, N., & Sitnov, M. (2005). Modeling the dynamics of the inner magnetosphere during strong geomagnetic storms. *Journal of Geophysical Research*, 110(A3), A03208. <https://doi.org/10.1029/2004JA010798>
- Usanova, M., Mann, I., Bortnik, J., Shao, L., & Angelopoulos, V. (2012). THEMIS observations of electromagnetic ion cyclotron wave occurrence: Dependence on AE, SYMH, and solar wind dynamic pressure. *Journal Geophysical Research*, 117. <https://doi.org/10.1029/2012JA018049>
- Usanova, M., Mann, I., Rae, I., Kale, Z., Angelopoulos, V., Bonnell, J., et al. (2008). Multipoint observations of magnetospheric compression-related EMIC Pc1 waves by THEMIS and CARISMA. *Geophysical Research Letters*, 35(17), L17S25. <https://doi.org/10.1029/2008GL034458>
- Yando, K., Millan, R. M., Green, J. C., & Evans, D. S. (2011). A Monte Carlo simulation of the NOAA POES medium energy proton and electron detector instrument. *Journal Geophysical Research*, 116, A10231. <https://doi.org/10.1029/2011JA016671>